Progress In Electromagnetics Research C, Vol. 128, 143–154, 2023

Microstrip Feed Line Characterization for Parabolic Reflector Antenna System Using Open-Loop Characterization Approach

Oluwole J. Famoriji* **and Thokozani Shongwe**

Abstract—Aperture efficiency determines the percentage of radiation power incident upon the antenna available at the feed-point. Because the geometry of reflector is fixed, the behavior is primarily a function of the feed. The feed line that connects (transmit/receive) RF to the feed becomes an integral part of the system, so achieving maximum aperture efficiency depends on the capacity of feed line. This paper proposes a microstrip feed line behavioral model for parabolic reflector antenna systems, using an open loop characterization approach. The dielectric loss of material varies based on material type. This is consequently used for the effective design of feed line, because the transmission line characteristic impedance varies based on material type and properties. This causes the reflection loss because of the mismatched impedance at both source and load. Loss tangential factor of a material type has notable impact on the loss profile. The developed model is analyzed with losses of the feed pattern and the distance between the edge and the vertex. The proposed attenuation factor can be used to predict loss intensity per feed line length, at different terrestrial and satellite communications frequency bands.

1. INTRODUCTION

Reflectors are important in satellite and terrestrial communication engineering because they exhibit high gains and simple geometry. Since geometry is fixed, the performance primarily depends on the feed. The most popular type of antenna in satellite communications is the parabolic reflector with horn feed [1] (Fig. 1). It has high gain and low cost of fabrication. The reflector cum complex mechanisms for mechanical beam steering is mobile usage useful such as *Intellian GX60* for *GlobalXpress* and 4-axis gimbal from *C2SAT* for *Ku*-band utilizations [2]. Electronic beam scanning has been developed for

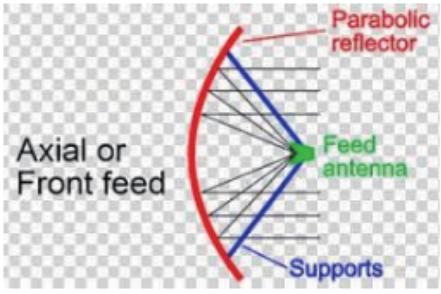

Figure 1. Parabolic reflector antenna configuration.

Received 2 November 2022, Accepted 14 December 2022, Scheduled 5 January 2023
* Corresponding author: Oluwole J. Famoriji (famoriji@mail.ustc.edu.cn).
The authors are with the Department of Electrical and Electronic Engineering Science, University of Johannesburg, P. O. Box 524, Auckland Park, Johannesburg 2006, South Africa.

ESOMPs for high-speed scanning and potentially flat designs. Various technical remedies have been proposed for Satcom such as phased array [2] and digital beamforming [3]. However, scanning range and large aperture give rise to many elements in the array, which are consequently costly remedies. The problems have potential solutions using metamaterials [4].

The feeds are usually coaxial or feed horn waveguides in prime focus reflectors [5, 6] situated at the focal point of reflector. Conversely, feed assembly increases reflector blockage, making the gain and radiation patterns worse. The feed supporting struts can also deteriorate the side lobe and cross-polarization levels. A possible way of resolving these issues is the employment of rear-radiating feeds, such as ring feed [7, 8], cup feed [9], hat feed [10, 11], and splash plate feed [12, 13]. They all suffer from limitation associated with their geometry. Microstrip antenna (Fig. 2) has simpler geometry, light weight, and smaller size, much easier to be integrated with electronics, and can be adapted into monolithic and hybrid integrated circuit fabrication at microwave frequencies [14]. Hence, microstrip feed is more beneficial due to the salient points stated above [15]. Microstrip transmission line (feed line) modeling becomes important for adequate design.

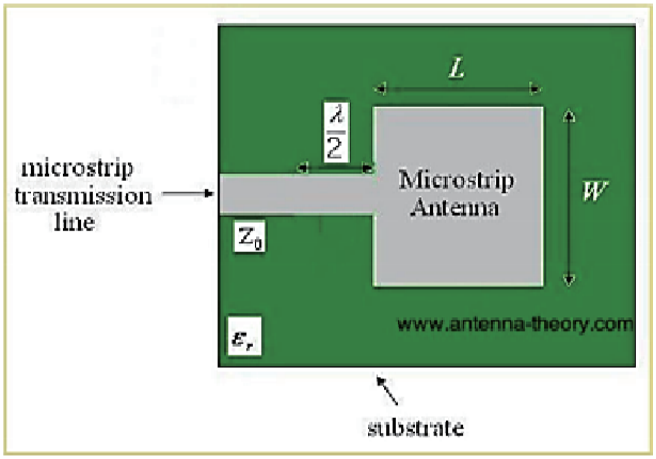

Figure 2. Microstrip antenna with microstrip feed line.

Increasing demand for high data-rate communications has greatly increased over the past decade. Having a reliable communication link, efficient feed-line which connects (transmitting/receiving) radio with antenna becomes important in order not to under illuminate reflector (wastage aluminium) or over illuminate (wastage of RF at the edges). Adequate knowledge of the total attenuation intensity profile of reflector system will help to design and come up with a cost effective and efficient signal feed and possibly enhance the choice of N-array for particular applications. Signal field strength and aperture efficiency at the reflector edge relative to the vertex because of the path length and feed pattern between the vertex and the edge have been accounted for and well documented by [16], but the feed line through which RF gets to the feed is neglected. Feed can suffer limitation if its transmission line (feed line) is not efficient. This work therefore proposes an improved model that incorporates feed line loss for present and future efficient terrestrial and satellite communications with a particular reference to microstrip transmission line. The model gives the knowledge of total loss in parabolic reflector system so as to achieve maximum reflector efficiencies practically targeted between 65 and 80% [17, 18]. In the time past, some reflector antennas have been designed [18, 20, 21], without attention on the feed line through which the antenna feed transmits/receives RF.

Other part of this paper is organized as follows. In Section 2, the parabolic reflector system analysis is presented. Aperture efficiency gives the percentage of radiation power incident upon the antenna that is available at the feed-point. Parabolic reflector antenna system feed line modeling is given in Section 3. A detailed modeling of general feed line is proposed which can be curve fitted for different feeding line techniques. Section 4 investigates thin-film microstrip line model and analysis, and the proposed total attenuation for parabolic reflector system is presented. The paper is concluded in Section 5.

2. PARABOLIC REFLECTOR SYSTEM ANALYSIS

This section examines the dependency of directivity and aperture efficiency on the primary-feed pattern $G_f(\theta', \phi')$ and f/d reflector ratio. For this analysis, we assume the circularly polarized feed pattern (i.e., does not depend on ϕ') and that $G_f(\theta', \phi') = 0$ for $\phi' > 90°$. The secondary pattern originated from the reflector surface is given as [17, 18]

$$\begin{bmatrix} E_\theta \\ E_\phi \end{bmatrix} = -j\frac{\omega\mu}{2\pi r}\sqrt{\frac{\epsilon}{\mu}}C_1 e^{-jkr}\begin{bmatrix} \hat{a}_\theta & .I \\ \hat{a}_\phi & .I \end{bmatrix} \tag{1}$$

By appropriation of current I, the E-field in the $\theta = \pi$ direction is given by either E_θ or E_ϕ. For circularly symmetric feed, linearly polarized in y-axis, and for negligible cross polarization, then Eq. (1) is reduced to

$$E(r, \theta = \pi) = -j\frac{2\omega\mu f}{r}\left[\sqrt{\frac{\epsilon}{\mu}}\frac{P_t}{2\pi}\right]^{\frac{1}{2}} e^{-jk(r+2f)}\int_0^{\theta_0}\sqrt{G_f(\theta', \phi')}\tan\left(\frac{\theta'}{2}\right)d\theta' \tag{2}$$

Power intensity, i.e., the forward direction power/unit solid angle $U(\theta = \pi)$, can be expressed as

$$U(\theta = \pi) = \frac{1}{2}r^2\sqrt{\frac{\epsilon}{\mu}}|E(r, \theta = \pi)|^2 \tag{3}$$

Substituting (2) into (3) then

$$U(\theta = \pi) = \frac{16\pi^2}{\lambda^2}f^2\frac{P_t}{4\pi}\left|\int_0^{\theta_0}\sqrt{G_f(\theta')}\tan\left(\frac{\theta'}{2}\right)d\theta'\right|^2 \tag{4}$$

The forward direction directivity of antenna can be expressed as [17, 18]:

$$D_0 = \frac{4\pi U(\theta = \pi)}{P_t} = \frac{U(\theta = \pi)}{P_t/4\pi} = \frac{16\pi^2}{\lambda^2}f^2\frac{P_t}{4\pi}\left|\int_0^{\theta_0}\sqrt{G_f(\theta')}\tan\left(\frac{\theta'}{2}\right)d\theta'\right|^2 \tag{5}$$

$$f = \left(\frac{d}{4}\right)\cot\left(\frac{\theta_0}{2}\right) \tag{6}$$

Focal length has a relationship with angular spectrum diameter d by Eq. (6), and Eq. (5) is reduced to:

$$D_0 = \left(\frac{\pi d}{\lambda}\right)^2\left\{\cot^2\left(\frac{\theta_0}{2}\right)\left|\int_0^{\theta_0}\sqrt{G_f(\theta')}\tan\left(\frac{\theta'}{2}\right)d\theta'\right|^2\right\} \tag{7}$$

Factor $\left(\frac{\pi d}{\lambda}\right)^2$ represents the directivity of a constant phase aperture that is uniformly illuminated, and other portion of the equation is the aperture efficiency expressed as [17, 18]

$$\epsilon_{ap} = \cot^2\left(\frac{\theta_0}{2}\right)\left|\int_0^{\theta_0}\sqrt{G_f(\theta')}\tan\left(\frac{\theta'}{2}\right)d\theta'\right|^2 \tag{8}$$

Apparently, aperture efficiency depends on the feed pattern $G_f(\theta')$ of a reflector and subtended angle θ_0. Therefore, for a feed pattern, paraboloids having equal f/d possess similar aperture efficiency [21–18]. The changes in the aperture efficiency based on the feed pattern and reflector angular extent according to a set of feeds with patterns are expressed as [17, 18]

$$G_f(\theta') = \begin{cases} G_0^n\cos^n(\theta'), & 0 \le \theta' \le \dfrac{\pi}{2} \\ 0, & \dfrac{\pi}{2} < \theta' \le \pi \end{cases} \tag{9}$$

G_0^n denotes the constant value for particular n. The patterns were selected because of the achievable closed form solutions and frequently used for the representation of a main section of the main lobe of different antennas in practice. Back region ($\frac{\pi}{2} < \theta' \le \pi$) intensity was taken as zero for the

prevention of interference between the direct feed radiation and the reflector-scattered radiation. G_0^n can be determined from the expression:

$$\oiint_s G_f\left(\theta'\right) d\Omega = \oiint_s G_f\left(\theta'\right) \sin\theta' d\phi' = 4\pi \tag{10}$$

By substitution it becomes:

$$G_0^n \int_0^{\pi/2} \cos^n\theta' \sin\theta' d\theta' = 2 \tag{11}$$

$$G_0^n{=}2(n+1)$$

The variation in the aperture efficiency depends on angular aperture of the reflector θ_0, shown in Fig. 3. It is evident that for a given feed pattern n, as n increases, the reflector angular aperture that gives rise to maximum efficiency becomes smaller, just a reflector having a specific angular aperture causes maximum aperture efficiency, and individual maximum aperture efficiency ranges *82–83%* and for any given patterns is almost equal to that of any of the others.

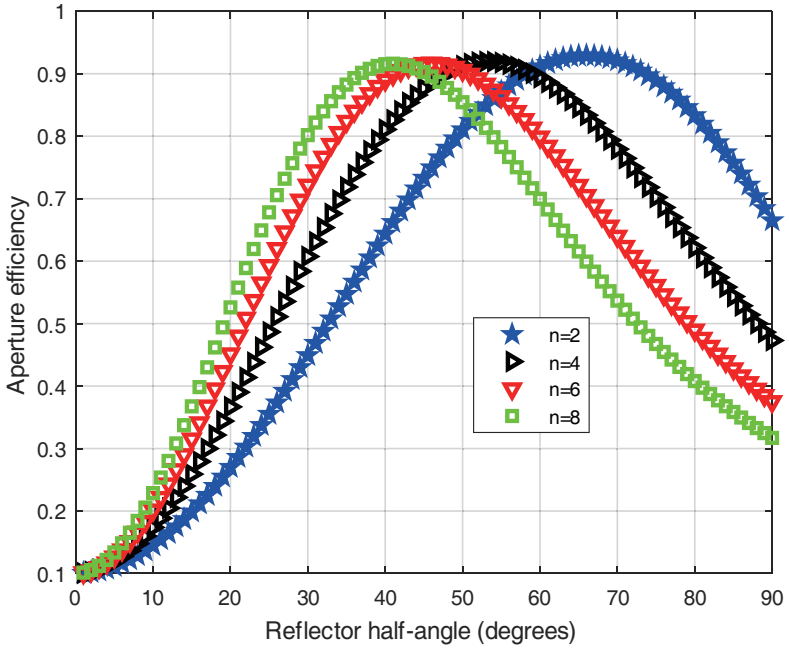

Figure 3. Aperture efficiency as a function of reflector half angle θ_0 for different feed pattern.

Aperture efficiency is the product of the spillover efficiency ϵ_s, tapper efficiency ϵ_t, phase efficiency ϵ_p, polarization efficiency ϵ_x, blockage efficiency ϵ_b, and random error efficiency. Therefore in general

$$\epsilon_{ap} = \epsilon_s\epsilon_t\epsilon_p\epsilon_x\epsilon_b\epsilon_r. \tag{12}$$

For feed with no random surface error, no blockage, symmetrical pattern, no cross-polarized field components, and aligned phased centers; spillover and tapper efficiencies are the main factor that contribute to aperture efficiency since losses depend primarily on the feed pattern. ϵ_s and ϵ_t are given below

$$\epsilon_s = \frac{\int_0^{\theta_0} G_f\left(\theta'\right) \sin\theta' d\theta'}{\int_0^{\pi} G_f\left(\theta'\right) \sin\theta' d\theta'} \tag{13}$$

$$\epsilon_t = 2\cot^2\left(\frac{\theta_0}{2}\right)\frac{\left|\int_0^{\theta_0}\sqrt{G_f(\theta')}\tan\left(\frac{\theta'}{2}\right)d\theta'\right|^2}{\int_0^{\theta_0}G_f(\theta')\sin\theta' d\theta'} \tag{14}$$

Tapper and spillover efficiencies depending on the half angle of the reflector for different feed patterns are as shown in Fig. 4 (integration of (a) and (b) gives rise to (c)). This shows that the product of spillover efficiency and taper efficiency majorly determine aperture efficiency, and very high efficiency is achievable using a narrow beam pattern of small minor lobes at the detriment of a very low taper efficiency.

Practically, there are power losses associated with each efficiency but another parameter limiting the gain of antenna is antenna feed attenuation, which is particular with the transmission line. Therefore, the characterization and modeling of feed lines technique becomes important for adequate system design.

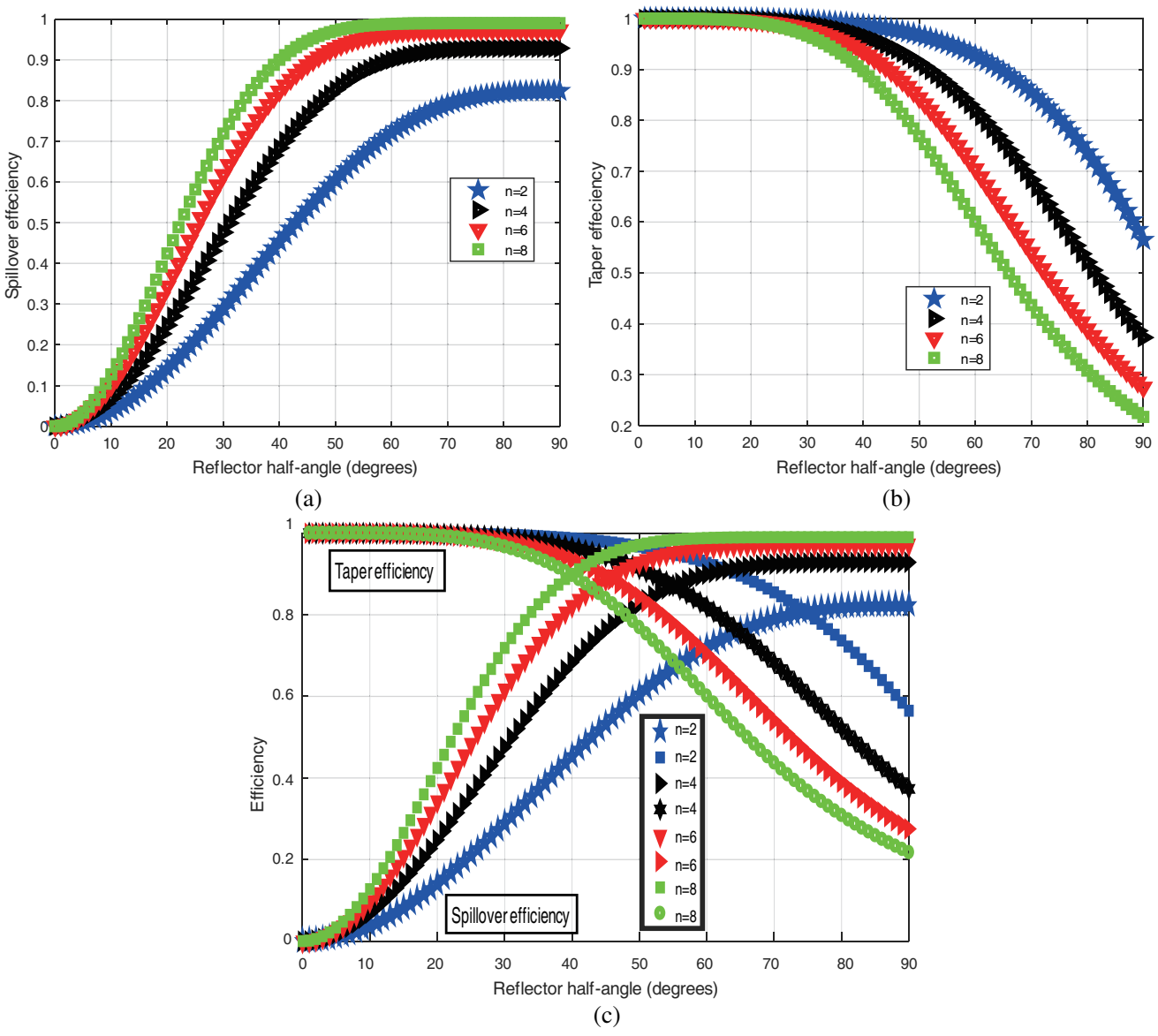

Figure 4. Taper (a) and spillover (b) efficiency depending on the half-angle of the reflector for various feed patterns. (c) Aperture efficiency as a product of taper and spillover efficiencies [17, 18].

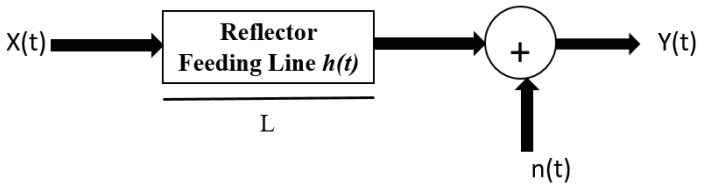

Figure 5. The system design.

3. FEED LINE MODELING OF PARABOLIC REFLECTOR ANTENNA SYSTEM

Antenna feed line is considered as an open loop system having both static and dynamic changes of the channel parameterized when being in use. Fig. 5 represents a typical open-loop system feeding line; $x(t)$ denotes the input signal; l is the length of the wireline; $h(t)$ is the response of the channel (feeding line); $n(t)$ is the noise; and $y(t)/l$ is the output signal received per length which is given as:

$$y\left(t\right)/l = h\left(t\right)x(t) + n\left(t\right) \tag{15}$$

Signal propagating along a wireline shares inverse relationship with a particular degree, m of its length, and signal intensity per length can be generally represented as [19]

$$\frac{y\left(t\right)}{x\left(t\right)} = \frac{K\lambda}{4\pi l^m} \tag{16}$$

where λ is the wavelength of the signal, and K is the constant of proportionality that defines links parameters and electrical resistivity ρ; ϵ_e is the effective dielectric constant defining the dielectric constant of a homogeneous medium that replaces air and dielectric regions of the microstrip of the wireline material, which depends on the type of the material, signal generator gain G_t, receiver gain G_m; K is

$$K = \epsilon_e \rho G_t G_m \tag{17}$$

where for a microstrip line [23]:

$$\epsilon_e = \frac{\epsilon_r + 1}{2} + \frac{\epsilon_r - 1}{2}\frac{1}{\sqrt{1 + \dfrac{12d}{W}}} \tag{18}$$

W is the width of conductor, d the thickness of the grounded dielectric substrate, and ϵ_r the relative permittivity. Since signal propagates via a medium and changes based on frequency, we introduce a factor gf^n. f is the frequency, and n and g account for other losses due to via-hole, bends, etc. of the feed line. Therefore, Eq. (4) is written as:

$$\frac{y/l}{x} = h = \frac{\epsilon_e \rho G_t G_r c}{4\pi \left(\dfrac{l}{l_0}\right)^m g \left(\dfrac{f}{f_0}\right)^n l_0^m f_0^n} \tag{19}$$

In practice, ideal environment does not exist, then $n > 0$. Assuming noise $n(t) = 0$, then, the received signal is expressed as

$$y\left(t\right)/l = \frac{\epsilon_e \rho G_t G_r c}{4\pi \left(\dfrac{l}{l_0}\right)^m g \left(\dfrac{f}{f_0}\right)^n l_0^m f_0^n} x(t) \tag{20}$$

$$P_r = \frac{P_t G_t G_r}{L_m} \tag{21}$$

Consequently, Eq. (5) predicts the signal intensity at any point. Hence, loss L_m and received signal are inversely related to each other (Eq. (7) [2]), and by substitution and logarithmic approach, loss gives:

$$L_m\left(dB/l\right) = L_{m0}\left(l_0, f_0, \rho, d, W, \epsilon_r\right) + 10m\log\left(\frac{l}{l_0}\right) + 10n\log\left(\frac{f}{f_0}\right) + P \tag{22}$$

where

$$L_{m0}\left(l_0, f_0, \rho, d, W, \epsilon_r\right) = 10\log\left(\frac{4\pi l_0^m f_0^n}{\left(\frac{\epsilon_r+1}{2} + \frac{\epsilon_r-1}{2}\frac{1}{\sqrt{1+\frac{12d}{W}}}\right)\rho c}\right) \tag{23}$$

frequency f is in Hz; the wireline length l can be in mm, μm, cm, etc. depending on applications; l_0 denotes the reference length; f_0 is in Hz; $L_{m0}\left(l_0, f_0, \rho, d, W, \epsilon_r\right)$ is the reference attenuation in dB; c is the speed of light (m/s); P is the distortion due to via hole, bends, etc. which is frequency dependent; ρ is the electrical resistivity of the wirelines such as coaxial feed line, microstrip feed line, and proximity coupled microstrip feed, which is usually constant. Losses due to transmission line that feeds the antenna have significant effect on the efficiency, therefore require attention for the modeling of signal attenuation or delay due to parasitic (RC and LC). The efficiency of the aperture and field intensity at reflector edge relative to the vertex due to the path length and feed pattern between the edge and vertex is given as

$$\text{Feed}\,(\text{dB}) \;=\; 10\log\left[G\left(\theta_0\right)\right] \tag{24}$$

$$\text{Path}\,(\text{dB}) \;=\; 10\log\left(\frac{r'}{f}\right)^2 \tag{25}$$

where f is the focal distance of the reflector, r' the distance from the focal point to the edge of the reflector, and θ_0 the reflector half angle. Eq. (24) accounts for the loss due to feed pattern while Eq. (25) describes the loss intensity between the edge and vertex of the reflector antenna system. Let L_m *(dB)* represent the attenuation intensity of the feed line, then the total attenuation A_{tot} can be expressed as

$$A_{tot} = 10\log\left[G\left(\theta_0\right)\right] + 10\log\left(\frac{r'}{f}\right)^2 + L_m \tag{26}$$

There are different feed line techniques available for reflector antenna to connect (transmitting/receiving) the associated radio frequencies, but microstrip feed line will be examined.

4. THIN-FILM MICROSTRIP LINE MODEL AND ANALYSIS

Thin-film microstrip lines (TFMSLs) are specially used in Si-based monolithic microwave integrated circuits (MMICs) and used as transmission line in multichip modules (MCMs) [24, 25]. The availability of high-quality polymers such as Benzocyclobutene (BCB), polymide as dielectric layers, makes the attenuation of TFMSLs likened to coplanar waveguides (CPWs) in GaAs MMICs. Also because transversal dimensions are scalable, miniaturized TFMSLs show excellent low-dispersive properties, and it is useable at sub-millimeter-wave range. The differences in geometrical dimensions: width, height, thickness, and conductivity of metallization cause a degree of discrepancies in the electrical response of signal conductor. Our model was tested against a robust TFMSL *(BCB with* $\epsilon_r = 2.7$ *and* $\tan\delta_z = 0.015$*;* $W = 8\,\mu m$*,* $h_s = 1.7\,\mu m$*,* $d = 0.8\,\mu m$*,* $Wg = 8\,\mu m$; conductivity of metalization $k = 2.5 \times 10^7\,\text{S/m}$) full wave EM simulation data in Fig. 6 of [24, 25]; result obtained is as shown in Fig. 6. P-values against the corresponding frequencies behavior and curve fitting response of P-function are as shown in Fig. 7, respectively. The model parameters are as summarized in Table 1 with Eq. (26). With this condition, our model can replace the complex one in [24–26]. This model is derived from stochastic point of view and can be easily implemented in common software tools. It is appropriate for conventional microstrip structure as well. The frequency range of application for thin-film microstrip lines (TFMSLs) can be extended down to dc level, and upper limit reaches submillimeter-wave range.

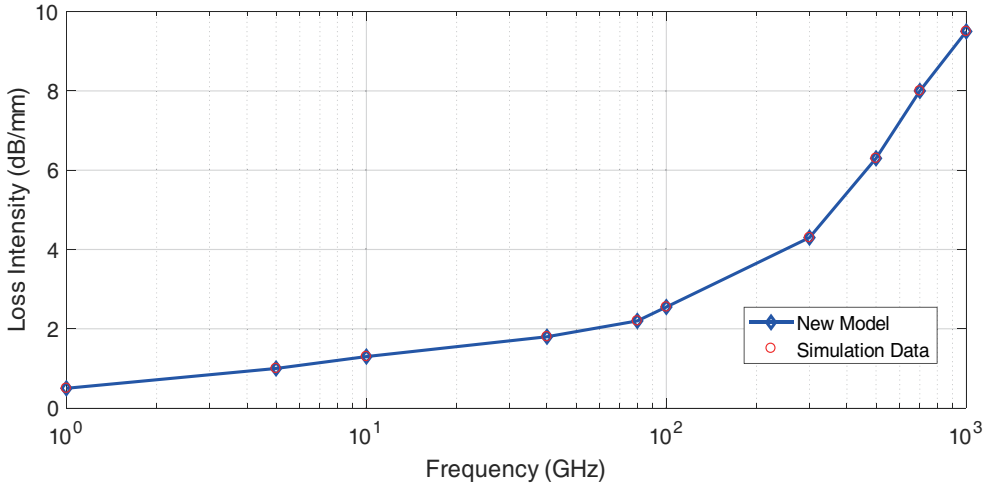

Figure 6. Model against EM simulation data.

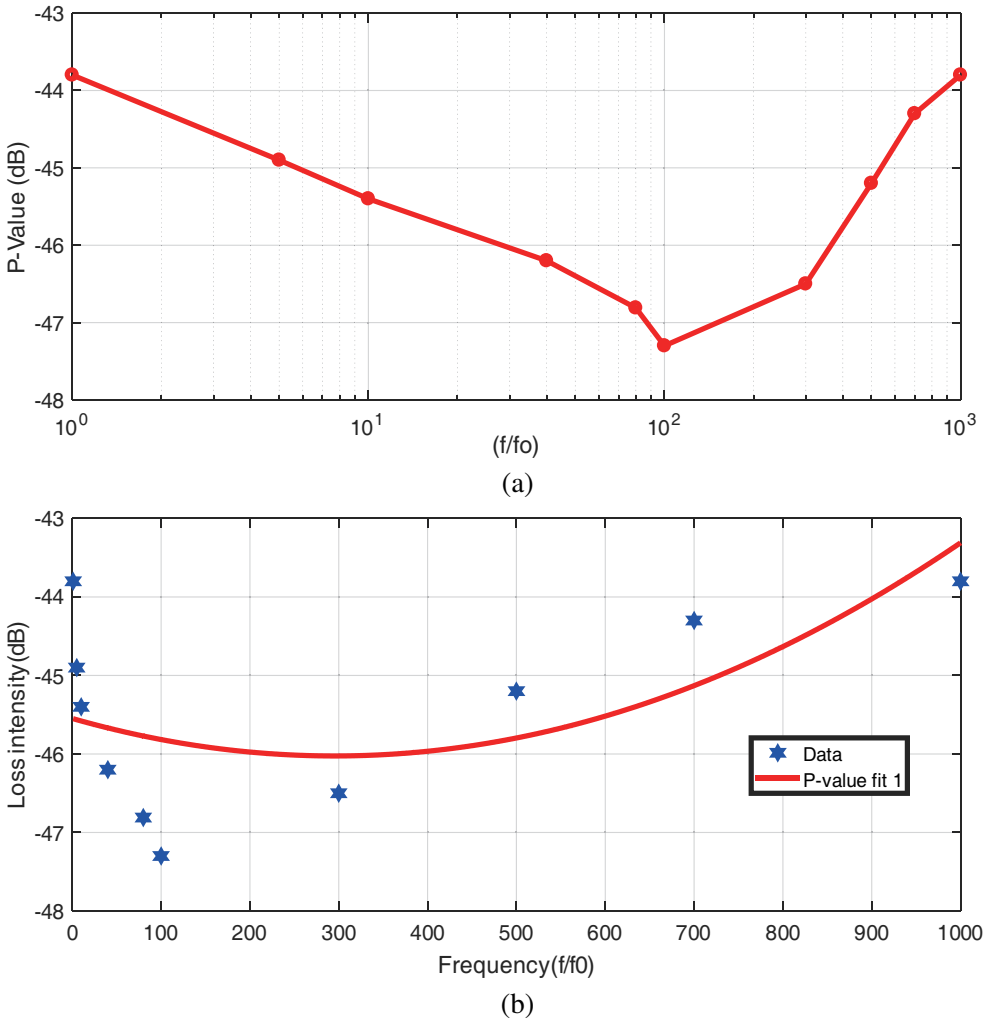

Figure 7. P-values against frequencies and curve fitting response.

Table 1. Microstrip line fitting parameter.

Parameter	m	n	α_o	α_1	α_2
Value	*1*	*0.3*	-45.55	-0.003	$5.5E^{-6}$

$$P = \alpha_o + \alpha_1 \log\left(\frac{f}{f_o}\right) + \alpha_2 \left(\log\left(\frac{f}{f_o}\right)\right)^2 \tag{27}$$

Simulation test results conducted between [25] and developed model (L_m) are presented in Fig. 8. The proposed model is faster in prediction and a good tool for microstrip feed line or interconnect loss/attenuation estimation. Relative permittivity effect of different materials; beeswax, gallium arsenide, paraffin, silicon and vaseline (all at 10 GHz) were tested with thickness $d = 0.01$ mm and width $W = 0.03$ mm, and the results are depicted in Fig. 9. The dielectric material loss changes from material to material, which should be considered for efficient feed line designs. The characteristic impedance of transmission line varies based on the type of material and the material properties (such as thickness and width); this causes reflection loss due to impedance mismatched at the source and load. Loss tangential factor of each material also has significant effect on the loss profile. Modifying feed line will enhance its impedance bandwidth for specific designs.

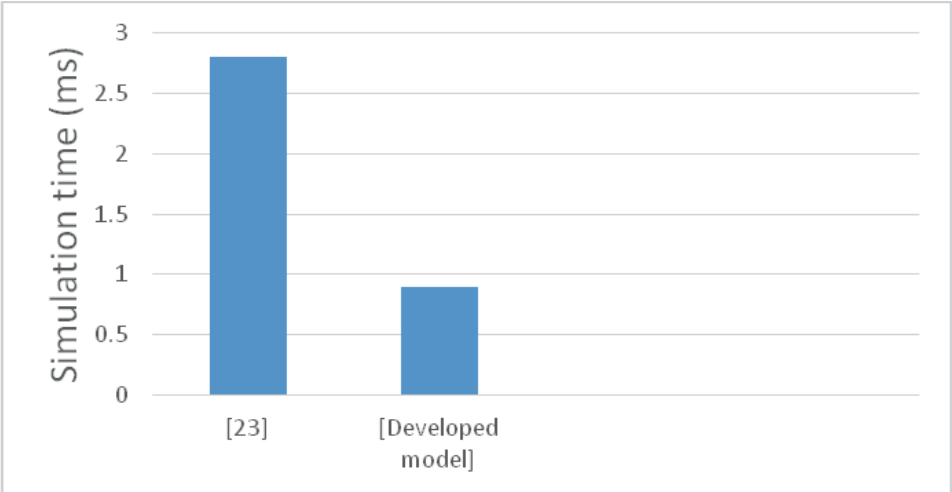

Figure 8. Simulation test result between [25] and developed model.

For primary parabolic reflector feed pattern ($n = 8$), $Feed(dB) = 10\log[G(\theta_0)] = -9.7776$ and $Path\ length\,(dB) = 10\log\left(\frac{r'}{f}\right)^2 = 1.137$ (this is in accordance with the simulation result of Fig. 3, also presented in [5]) with silicon dielectric material, the proposed model for parabolic reflector antenna system (A_{tot}) in Eq. (26) was simulated for prediction at various satellite communication bands ranging from L-band to Ka-band, and the result obtained is as presented in Fig. 10. It could be said that [5] and [17] are under estimated total loss because feed line was not considered at all. Feed line loss is part of the system and should be considered for optimum design. Microstrip feed line in parabolic reflector has been examined, and an empirical model is proposed to replace the conventional approach (S-parameter data from EM-simulation tool), in addition to losses due to path length and feed pattern. This will enhance the development of parabolic reflector antenna systems employing microstrip feed line for present/future terrestrial and satellite communications.

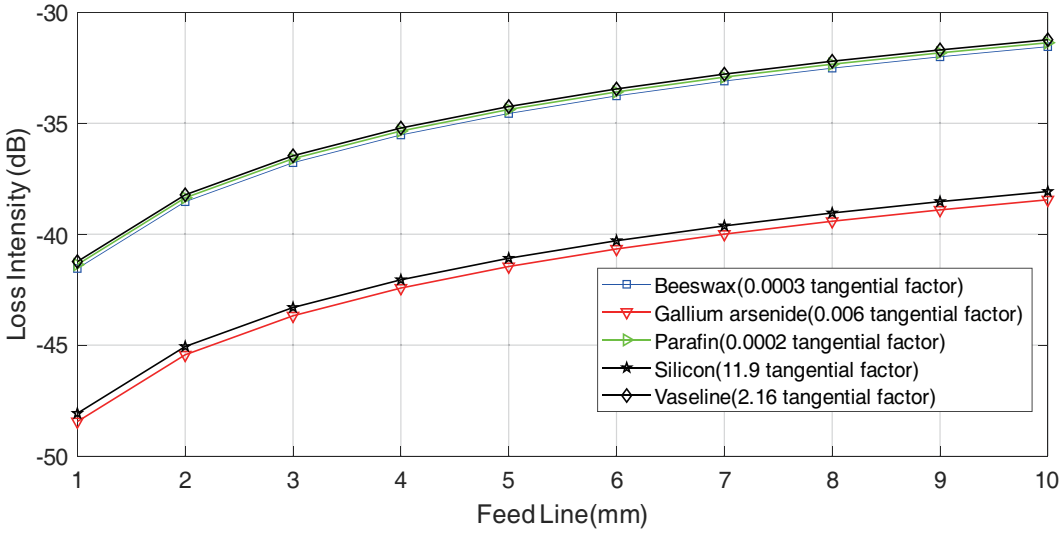

Figure 9. Feed line dielectric material dependency of the model (L_m) at *10 GHz* and 25°C.

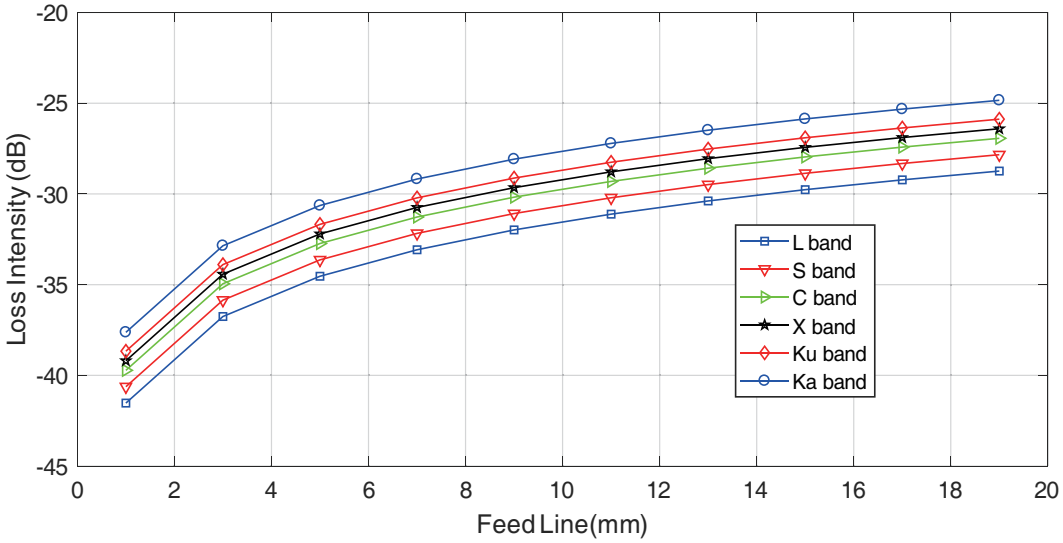

Figure 10. Parabolic reflector antenna system loss intensity profile.

5. CONCLUSION

In this paper, a microstrip feed line behavioral model has been developed and evaluated for parabolic reflector antenna system application towards efficient terrestrial and satellite communications using an open-loop characterization approach. Feed line loss with loss due to feed pattern and path length between the edge and the vertex of reflector are useful considerations to attain maximum aperture efficiency. The dielectric loss of material varies based on material type. This is consequently used for the effective design of feed line, because the transmission line characteristic impedance varies based on material type and properties. This causes the reflection loss because of the mismatched impedance at both source and load. Loss tangential factor of a material type has notable impact on the loss profile. The developed model was analyzed with losses associated with feed pattern and the path length between the edge and vertex. The proposed model aids the knowledge and prediction of essential performance of both present and future applications of parabolic reflector antenna systems with microstrip feed line.

REFERENCES

1. Rohrdantz, B., T. Jaschke, T. Reuschel, S. Radzijewski, A. Sieganschin, and A. F. Jacob, "An electronically scannable reflector antenna using a planar active array feed at Ka-band," *IEEE Trans. Microw. Theory Techn.*, Vol. 65, No. 5, 1650–1661, May 2017.
2. Dubok, A., G. Gerini, A. B. Smolders, "Extreme scanning double shape-reflector antenna with multiple interactions for focal plane array applications," *IEEE Trans. Antenna Prop.*, Vol. 68, No. 7, 5686–5690, Jan. 2020.
3. Wu, Q., X. Jiang, and C. Zhang, "Attenuation of orbital angular momentum beam transmission with a parabolic antenna," *IEEE Antennas Wireless Propag. Lett.*, Vol. 20, No. 10, 1849–1853, Jul. 2021.
4. Rohrdantz, B., K. Kuhlmann, A. Stark, A. Geise, and A. F. Jacob, "Digital beamforming antenna array with polarization multiplexing for mobile high-speed satellite terminal at Ka-band," *J. Eng.*, Vol. 1, No. 1, 9, Feb. 2016.
5. Famoriji, O. J., S. Yang, Y. Li, W. Chen, A. Fadamiro, Z. Zhang, and F. Lin, "Design of a simple circularly polarized dual-frequency reconfigurable microstrip patch antenna array for millimeter-wave applications," *IET Microwave, Antennas & Propagation*, Vol. 13, No. 10, 1671–1677, Aug. 2019.
6. Debbarma, K., N. Truong, S. K. Sharma, and J. S. Chieh, "2-D beam steering performance of a triple mode horn antenna integrated with risley prism and phase correcting surface," *IEEE Open Journal of Antennas Prop.*, Vol. 3, 752–761, Jun. 2022.
7. Clarricoats, P. J. B. and A. D. Olver, "Corrugated horns for microwave antennas," *Peter Peregrinus*, London, U.K., 1994.
8. Kildal, P. S. and S. A. Skyttemyr, "Dipole-disk antenna with beam-forming ring," *IEEE Trans. Antennas Propag.*, Vol. 30, No. 4, 529–534, 1982.
9. Cutler, C. C., "Parabolic-antenna design for microwaves," *Proc. IRE*, Vol. 35, No. 11, 1284–1294, 1947.
10. Poulton, G. T. and T. S. Bird, "Improved rear-radiating waveguide cup feeds," *Proc. IEEE Antennas Propag. Int. Symp.*, Mill Valley, CA, Vol. 1, 79–82, 1986.
11. Famoriji, O. J., K. F. Akingbade, E. O. Ogunti, W. Apena, A. Fadamiro, and F. Lin, "Analysis of phased array antenna system via spherical harmonics decomposition," *IET Communications*, Vol. 13, No. 18, 3097–3104, Nov. 2019.
12. Hansen, J., A. A. Kishk, P.S. Kildal, and O. Dahlsjo, "High performance reflector hat antenna with very low sidelobes for radio-link applications," *Proc. Antennas Propag. Soc. Int. Symp.*, Vol. 2, 893–896, 1995.
13. James, G. L. and D. P. S. Malik, "Towards the theoretical design of splash-plate feeds," *Electron. Lett.*, Vol. 11, No. 24, 593–594, 1975.
14. Newham, P., "A high efficiency splash plate feed for small reflector antennas," *Proc. IEEE Antennas Propag. Int. Symp.*, 420–423, 1985.
15. Pozarand, D. M. and D. Schaubert, "Microstrip antennas: the analysis and design of microstrip antennas and arrays," *Institute of Electrical Engineers*, London, U.K., 1994.
16. Qudrat-E-Maula, M. and L. Shafai, "Low-cost, microwave-fed printed dipole for prime focus reflector feed," *IEEE Trans. Antenna Prop.*, Vol. 60, No. 11, 5428–5433, Nov. 2012.
17. Love, A. W., "Reflector antennas," *IEEE Press*, New York, 1978.
18. Balanis, C. A., "Antenna theory, analysis and design," *John Wiley & Sons, Inc.*, 3rd Edition, Hoboken, New Jersey, 2005.
19. Famoriji, O. J., X. Yan, M. Khan, R. Kashif, A. Fadamiro, Md S. Ali, and F. Lin, "Wireless interconnect in multilayer chip-area-network for future multimaterial high-speed," *Wireless Communications and Mobile Computing*, Vol. 2017, Article ID 6083626, 2017.
20. Rahmat-Samii, Y. and R. Haupt, "Reflector antenna developments: A perspective on the past, present and future," *IEEE Antennas Propag. Mag.*, Vol. 57, No. 2, 85–95, Sep. 2015.

21. Ivashina, M. V., M. N. M. Kehn, P Kildal, and R. Maaskant, "Decoupling efficiency of a wideband Vivaldi focal plane array feeding a reflector antenna," *IEEE Trans. Antenna Prop.*, Vol. 57, No. 12, 373–382, Feb. 2009.
22. Hosseini, A., S. Kabiri, and F. D. Flaviis, "V-band high-gain printed quasi-parabolic reflector antenna with beam-steering," *IEEE Trans. Antenna Prop.*, Vol. 65, No. 4, 1589–1598, Apr. 2017.
23. Silver, S., "Microwave antenna theory and design," *McGraw-Hill MIT Radiation Lab. Series*, Vol. 12, New York, 1949.
24. Famoriji, O. J., X. Yan, M. Khan, R. Kashif, A. Fadamiro, Md S. Ali, and F. Lin, "Wireless interconnect in multilayer chip-area-network for future multimaterial high-speed," *Wireless Communications and Mobile Computing*, Vol. 2017, Article ID 6083626, 2017.
25. Pozar, D. M., "Microwave engineering," *John Wiley and Sons, INC*, 2nd Edition, 1998.
26. Schnieder, F. and W. Heinrich, "Model of thin-film microstrip line for circuit design," *IEEE Trans. on Microwave Theory and Techn.*, Vol. 49, 104–110, Jan. 2001.